

# Human memory CD8 T cell effector potential is epigenetically preserved during in vivo homeostasis

Hossam A. Abdelsamed,<sup>1</sup> Ardiana Moustaki,<sup>1</sup> Yiping Fan,<sup>2</sup> Pranay Dogra,<sup>1</sup> Hazem E. Ghoneim,<sup>1</sup> Caitlin C. Zebley,<sup>1,3</sup> Brandon M. Triplett,<sup>4</sup> Rafick-Pierre Sekaly,<sup>5</sup> and Ben Youngblood<sup>1</sup>

<sup>1</sup>Department of Immunology, <sup>2</sup>Department of Computational Biology, <sup>3</sup>Department of Oncology, and <sup>4</sup>Department of Bone Marrow Transplantation and Cellular Therapy, St. Jude Children's Research Hospital, Memphis, TN 38105

<sup>5</sup>Department of Pathology, Case Western Reserve University, Cleveland, OH 44106

**Antigen-independent homeostasis of memory CD8 T cells is vital for sustaining long-lived T cell-mediated immunity. In this study, we report that maintenance of human memory CD8 T cell effector potential during in vitro and in vivo homeostatic proliferation is coupled to preservation of acquired DNA methylation programs. Whole-genome bisulfite sequencing of primary human naive, short-lived effector memory ( $T_{EM}$ ), and longer-lived central memory ( $T_{CM}$ ) and stem cell memory ( $T_{SCM}$ ) CD8 T cells identified effector molecules with demethylated promoters and poised for expression. Effector-loci demethylation was heritably preserved during IL-7- and IL-15-mediated in vitro cell proliferation. Conversely, cytokine-driven proliferation of  $T_{CM}$  and  $T_{SCM}$  memory cells resulted in phenotypic conversion into  $T_{EM}$  cells and was coupled to increased methylation of the CCR7 and Tcf7 loci. Furthermore, haploidentical donor memory CD8 T cells undergoing in vivo proliferation in lymphodepleted recipients also maintained their effector-associated demethylated status but acquired  $T_{EM}$ -associated programs. These data demonstrate that effector-associated epigenetic programs are preserved during cytokine-driven subset interconversion of human memory CD8 T cells.**

## INTRODUCTION

Immunological memory is a cardinal feature of adaptive immunity that provides a significant survival advantage by protecting individuals from previously encountered pathogens (Plotkin et al., 2013). Memory CD8 T cells have the potential to provide lifelong protection against pathogens containing their cognate epitope and are currently being exploited for strategies to protect against various intracellular pathogens and tumors. To achieve such long-lived protection, an adequate number of functionally competent memory CD8 T cells must be sustained in the absence of antigen through cytokine-driven homeostatic proliferation (Vella et al., 1997; Lodolce et al., 1998; Wong and Pamer, 2001; Becker et al., 2002, 2005; Goldrath et al., 2002; Tan et al., 2002; Kaech et al., 2003). Such homeostasis-promoting cytokines enable a slow but continuous level of proliferation that does not appear to compromise the ability of memory CD8 T cells to rapidly recall their effector functions. Yet the cell-intrinsic mechanisms that maintain acquired memory-associated effector functions remain poorly defined.

A defining feature of T cell memory is the ability to rapidly transition from a quiescent state to a highly proliferative, cytolytic population of effector cells upon antigen reexposure (Zimmermann et al., 1999; Veiga-Fernandes et al., 2000). However, the specific capacity for mounting such a response in terms

of proliferation, tissue homing, and recall of effector function is disproportionately attained by different subsets of memory T cells (Hamann et al., 1997; Sallusto et al., 1999; Gattinoni et al., 2011). The phenotypic heterogeneity among the pool of memory T cells can be partitioned into subsets with distinct tissue homing and proliferative potential based on the expression of the lymphoid-homing chemokine receptor CCR7 (Sallusto et al., 1999). Distinguished by a CCR7<sup>+</sup> CD45RA<sup>-</sup> phenotype, the now commonly termed central memory ( $T_{CM}$ ) subset of CD8 T cells has increased access to lymphoid tissue, whereas effector memory ( $T_{EM}$ ) CCR7<sup>-</sup> CD45RA<sup>-</sup> CD8 T cells home to nonlymphoid tissues (Sallusto et al., 1999; Masopust et al., 2001; Lefrançois and Masopust, 2002). Recently, a new subset of human memory CD8 T cells was identified based on expression of the surface markers CD95 and CD122. These memory T cells share many phenotypic properties with naive T cells, but unlike naive cells, they possess a heightened capacity to undergo IL-7- and IL-15-driven homeostatic proliferation (Gattinoni et al., 2011). Moreover, this subset of memory cells exhibits the greatest level of cytokine-driven, homeostatic proliferation compared with that of other, more conventional, memory subsets. Given their tremendous ability to self-renew and give rise to other memory subsets, these cells are referred to as stem cell memory ( $T_{SCM}$ ) CD8 T cells.

Downloaded from [http://jpress.org/jem/article-pdf/214/6/1593/1758189/jem\\_20161760.pdf](http://jpress.org/jem/article-pdf/214/6/1593/1758189/jem_20161760.pdf) by guest on 09 February 2020

Correspondence to Ben Youngblood: benjamin.youngblood@stjude.org

Abbreviations used: DMR, differentially methylated region; IPA, ingenuity pathway analysis; PCA, principal component analysis; WGBS, whole-genome bisulfite sequencing.



Similar to stem cells, memory CD8 T cells face the challenge of balancing cell-fate stability, which is required for long-term homeostasis of subset specification, with the plasticity required for antigen-triggered cell differentiation during a recall response. Several studies addressing the underlying mechanisms of memory T cell differentiation have revealed that many of the phenotypic and functional adaptations among memory T cell subsets manifest at the level of transcriptional regulation (Gattinoni et al., 2011; Thaventhiran et al., 2013; Tzelepis et al., 2013). For instance, the poised ability to recall effector molecules, including IFN $\gamma$ , perforin (Prf1), and granzyme B (GzmB), is accompanied by either a sustained, elevated level of transcription in the resting memory cells and/or a rapid induction of transcription upon TCR signaling (Weng et al., 2012). The poised state of these loci in memory CD8 T cells has been associated with an increased level of trimethylation of the H3K4 (permissive mark) and H3K27 (repressive mark) histones near the gene transcriptional start site (Araki et al., 2009; Weng et al., 2012; Russ et al., 2014), yet whether these epigenetic programs are sustained during homeostatic self-renewal remains unclear.

Maintenance of acquired transcriptional programming in a dividing population of differentiated cells is mediated through epigenetic modifications. Specifically, CpG DNA methylation and histone modification promote and maintain changes in chromatin accessibility that control transcriptional permissibility (Fitzpatrick et al., 1999; Araki et al., 2009). Although recent genome-wide studies of human memory CD8 T cells have reported specific correlations between gene expression and the density of different histone modifications (Araki et al., 2009; Denton et al., 2011), mounting evidence in other model systems suggests that DNA-methylation programming is a primary mediator for preserving transcriptionally repressive and permissive chromatin states in cells that have undergone several rounds of division (Katan-Khaykovich and Struhl, 2002; Jones, 2012; Bintu et al., 2016).

To determine whether changes in DNA methylation are coupled to the establishment and maintenance of memory-associated programs in human CD8 T cells, we performed a whole-genome assessment of DNA-methylation patterns in freshly isolated human naive and memory CD8 T cell subsets and tracked the stability of memory-associated epigenetic programs during *in vitro* cytokine-driven homeostatic proliferation and *in vivo* after infusion of haploidentical memory T cells into transplant patients. Here we show that human memory CD8 T cell-associated DNA methylation programs can be maintained during antigen-independent self-renewal. These data provide new insight into the molecular mechanism for maintenance of acquired functions in memory CD8 T cells during homeostasis and the future design of therapies to manipulate the antiviral and antitumor activities of those cells.

## RESULTS AND DISCUSSION

### Human memory CD8 T cell differentiation is coupled to subset-specific changes in DNA methylation

Homeostatic proliferation of memory CD8 T cells ensures preservation of T cell-based immunity by maintenance of a poised effector response for a long period of time. Maintenance of this state of readiness during cell division suggests the presence of a stable epigenetic mechanism, such as DNA methylation. However, it remains unclear whether DNA methylation programs acquired in long-lived memory CD8 T cells are maintained during antigen-independent proliferation. To determine whether memory-associated DNA methylation programs are maintained during homeostasis, we first sought to define bona fide memory subset-specific DNA methylation programs by performing whole-genome bisulfite sequencing (WGBS) of freshly isolated human naive and memory CD8 T cell subsets (Fig. 1 A).

Our initial assessment of genome-wide DNA methylation levels revealed that the overall number of methylated CpGs was inversely correlated with the established differentiation state of these cells: naive > T<sub>SCM</sub> > T<sub>CM</sub> > T<sub>EM</sub>. Moreover, the progressive decline in DNA methylation occurred across all autosomal chromosomes, indicating that effector and memory T cell differentiation is coupled to broad changes in DNA methylation (Fig. S1 B and Fig. 1 B). The variable levels of methylation among the long-lived versus short-lived memory CD8 T cell subsets prompted us to further assess the relationship between naive and memory CD8 T cell methylation profiles. An unsupervised principal component analysis (PCA) was performed on the methylation status of all CpG sites across the genome (Fig. 1 C). Clustering was observed among the naive replicates as well as among T<sub>SCM</sub> replicates, but notably, the naive and T<sub>SCM</sub> samples were found to be epigenetically distant (Fig. S1 C). Based on the methylation status at 9,377,480 CpGs (CpG sites with more than five times the sequencing coverage for every sample), we generated a dendrogram of all replicate samples. Calculation of Euclidean distances between each population in the dendrogram indicated that, despite the higher level of global DNA methylation, long-lived memory CD8 T cells (T<sub>SCM</sub>) have DNA methylation programs that are distinct from naive cells (Fig. S1 C).

To better define the DNA methylation programs that distinguish memory CD8 T cells from naive cells, we performed a pairwise comparison of naive versus memory cell WGBS datasets, identifying differences in DNA methylation at individual CpG sites across the genome. This comparison allowed us to define the number, distribution, and nature of differentially methylated regions (DMRs) between the genomes of naive and memory T cell subsets. We observed the greatest number of demethylated regions in T<sub>EM</sub> cells relative to naive T cells (Fig. 1 D, top), further indicating that the T<sub>EM</sub> memory subset is the most epigenetically distinct population from naive CD8 T cells (Fig. 1 B and Fig. S1 B). Regardless of the methylated-versus-demethylated status, most of

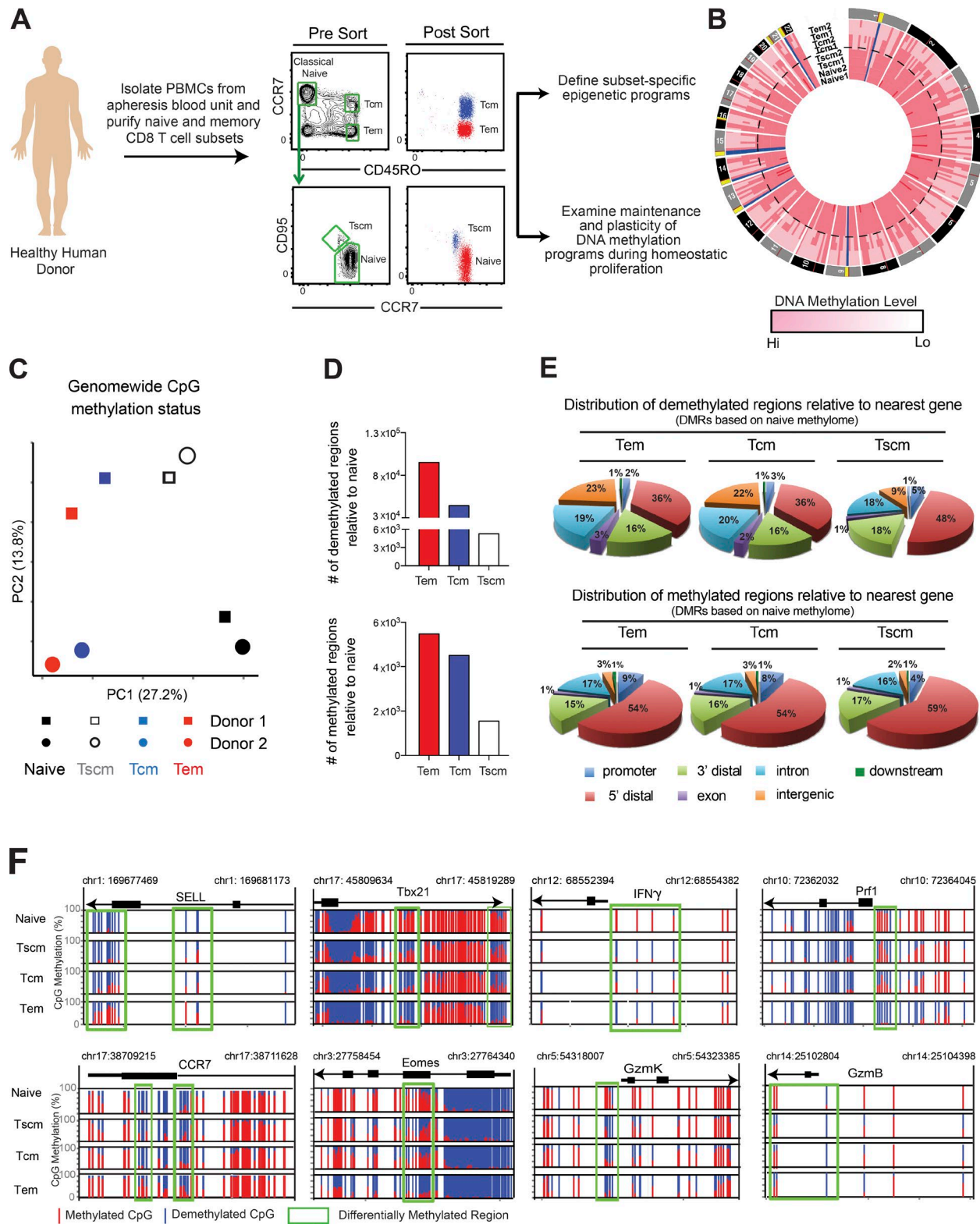


**Figure 1. Genome-wide changes in DNA-methylation programming are coupled to human memory CD8 T cell subset-specific differentiation.** (A) Flow cytometry-based strategy for isolating a sufficient quantity of naive and memory CD8 T cell subsets from apheresis blood unit of healthy donors for phenotypic, functional, and whole-genome epigenetic characterization. The cell subsets were identified based on the expression of three cell surface markers as follows: naive: CCR7<sup>+</sup>, CD45RO<sup>-</sup>, and CD95<sup>-</sup>; Tem: CCR7<sup>-</sup> and CD45RO<sup>+</sup>; Tcm: CCR7<sup>+</sup> and CD45RO<sup>+</sup>; Tscm: CCR7<sup>+</sup>, CD45RO<sup>-</sup>, and CD95<sup>+</sup>. (B) Circos

the DMRs were enriched in the 5'-distal (1–50 kb) regions, suggesting an association with the transcriptional regulatory regions. These results prompted us to compare our WGBS data to the published histone profiles in human T<sub>EM</sub> and T<sub>CM</sub> CD8 T cells (Araki et al., 2009). We found that these histone modifications (H3K4me3 and H3K27me3) only overlap with ~75% of the DMRs (methylated and unmethylated). Importantly, the remaining 25% of the DMRs that did not overlap with the published histone modifications were enriched in the 5' distal regions of genes (Fig. S1 D), which may represent enhancer elements. Indeed, a recent study by Charlet et al. (2016) demonstrated the coexistence of CpG methylation and H3K27ac in enhancers outside transcription factor-binding sites and correlated this coexistence with a decrease in chromatin accessibility. Thus, the WGBS methylation data provided in this study reveal a comprehensive profile of genomic regions undergoing epigenetic reprogramming during human memory T cell differentiation.

#### Effector and memory-associated genes are targeted for DNA methylation reprogramming during differentiation of memory T cells

We next sought to identify DNA methylation programs coupled to the unique properties of the individual memory T cell subsets. Again, a pairwise comparison of the methylation status among each memory subset was performed, and we detected 201,980, 62,240, and 9,026 DMRs unique to T<sub>EM</sub>, T<sub>CM</sub>, and T<sub>SCM</sub> CD8 T cells, respectively (Fig. S1 E). Among the DMRs that delineate the T<sub>EM</sub>, T<sub>CM</sub>, and T<sub>SCM</sub> CD8 T cells were subset-associated DMRs at CpG sites in the *CCR7* and *CD62L* (*SELL*) loci. Both *CCR7* and *CD62L* DMRs were significantly methylated in CD8 T<sub>EM</sub> cells, whereas these regions remained predominantly unmethylated in naive, T<sub>CM</sub>, and T<sub>SCM</sub> CD8 T cells, consistent with the relative level of expression of those molecules in the different cell subsets (Fig. 1, A and F). Similar to the lymphoid-homing molecules, we observed striking differences in methylation status at the transcription factor loci for T-bet (*Tbx21*), eomesodermin (*Eomes*) and T cell–specific transcription factor (*TCF7*, coding for the *Tcf1* protein; Fig. 1 F and Fig. S1 F), all of which have well-established roles in CD8 T cell effector and memory differentiation (Pearce et al., 2003; Intlekofer et al., 2005, 2007; Gattinoni et al., 2009; Banerjee et al., 2010; Pipkin et

al., 2010; Joshi et al., 2011). Consistent with the relative level of gene expression, all memory CD8 T cells were generally demethylated at regions downstream of the transcriptional start site of T-bet and Eomes relative to that in naive T cells (Fig. 1 F and Fig. S2, A and B). Notably, several genes with established roles in regulating cellular plasticity, including *DNMT3A* and *TCF7* (Chen et al., 2002; Gattinoni et al., 2009; Thomas et al., 2012), were progressively enriched for promoter methylation following a hierarchical order of least differentiated to most differentiated cells (naive < T<sub>SCM</sub> < T<sub>CM</sub> < T<sub>EM</sub>; Fig. S1, F and G). Collectively, these data suggest that changes in epigenetic programs that occur during memory T cell differentiation are coupled to memory T cell subset specification and plasticity.

In contrast to the memory subset-specific DNA methylation programs found at lymphoid homing molecules and transcription factors, demethylation DMRs at loci of classically defined effector molecules, including *IFN $\gamma$* , Perforin, *GZMB*, and *GZMK*, were observed in all memory T cell subsets (Fig. 1 F). Of particular note was the level of demethylation at these loci in the long-lived T<sub>SCM</sub> CD8 T cells. This observed state of epigenetic permissiveness is in striking contrast to a previous study examining in vitro–generated mouse T<sub>SCM</sub> CD8 T cells, which reported that effector loci retained an epigenetic program that was not transcriptionally permissive (Crompton et al., 2016). Importantly, these new data are consistent with the hypothesis that T<sub>SCM</sub> development may transit through an effector stage of cell differentiation.

To more broadly characterize DMRs linked to memory T cell longevity, we performed an ingenuity pathway analysis (IPA) of genes associated with naive versus T<sub>SCM</sub> CD8 T cell DMRs. The IPA upstream regulator analysis identified STAT3 as being among the top potential regulators of the T<sub>SCM</sub> DMR gene list (Fig. S1 H), further linking memory CD8 T cell development (Cui et al., 2011) and the epigenetic poising of effector functions in long-lived memory T cells. We further assessed the relationship between changes in DNA methylation and memory T cell longevity by analyzing DMRs between shorter-lived T<sub>EM</sub> and long-lived T<sub>SCM</sub> CD8 T cells. Notably, the top canonical pathways associated with the methylated and demethylated DMRs, between T<sub>EM</sub> and T<sub>SCM</sub> cells, were involved in cellular proliferation, including the anti-proliferative role of TOB (Transducer of *ERBB2*)

plot showing DNA methylation levels for naive and memory CD8 T cell subsets across the whole genome from two donors. CpG methylation levels were averaged over 10-Mb genomic intervals and are represented as histogram tracks. Heat map shows changes in the levels of DNA methylation with respect to the sample across the entire genome. Dark red indicates high levels of methylation, and light red indicates low levels of methylation. Dotted black circle separates two methylation patterns: dark red (high methylation, as in naive and T<sub>SCM</sub>) and light red (low methylation, as in T<sub>CM</sub> and T<sub>EM</sub>). (C) PCA of methylation status of total CpGs with more than five times the coverage. (D) Summary graph of the number of methylated and demethylated regions in the T<sub>EM</sub>, T<sub>CM</sub>, and T<sub>SCM</sub> genomes relative to that in the naive CD8<sup>+</sup> T cell genome. The number of demethylated regions was calculated based on difference  $\geq 30\%$  methylation between two populations. The number of methylated regions was calculated based on  $\leq 30\%$  methylation difference between the two populations. (E) Pie charts showing the percentage of demethylated and methylated regions across the genomes of T<sub>EM</sub>, T<sub>CM</sub>, and T<sub>SCM</sub> cells relative to that of naive CD8 T cells. (F) Normalized plot of CpG methylation at sites surrounding and within DMRs of effector molecules (*IFN $\gamma$* , *PRF1*, *GZMB*, and *GZMK*), tissue-homing molecules (*CD62L* and *CCR7*), and transcription factors (*T-BET* and *EOMES*) obtained from WGBS analysis. Red and blue lines depict methylation and demethylation of CpG sites, respectively.

in T cell signaling and LXR/RXR activation (Fig. S1 I), which has been associated with reduction in T cell proliferation (Bensinger et al., 2008). These data are consistent with  $T_{EM}$  having a reduced capacity for homeostatic proliferative capacity relative to  $T_{SCM}$  cells, and further indicate that the functional delineation among memory T cell subsets is coupled to changes in DNA methylation.

#### Demethylated effector loci in human memory CD8 T cells remain poised for expression during cytokine-driven proliferation

Having determined that the loci of several effector molecules in long-lived memory CD8 T cells contain an epigenetic program suggestive of transcriptional permissivity, we next sought to determine whether the effector-associated loci were poised for rapid gene expression in response to TCR stimulation. Naive and memory CD8 T cell subsets were purified and then cultured in the presence of anti-CD3/CD28 antibodies. mRNA was isolated longitudinally from the naive and memory CD8 T cell subsets at 0, 4, and 12 h after TCR stimulation, and the level of *IFN $\gamma$* , *GZMB*, and *PRF1* transcription was determined. Our results revealed that *GZMB* and *PRF1* transcription is rapidly induced in  $T_{CM}$  and  $T_{SCM}$  cells upon TCR ligation, whereas  $T_{EM}$  cells maintained a constitutively high level of expression after TCR activation (Fig. S3 A). Interestingly, the level of *IFN $\gamma$*  mRNA was high in all resting memory CD8 T cell subsets, relative to naive cells (Fig. S3 A) but was further up-regulated upon stimulation of the memory subsets. Similar to the heightened kinetics for gene expression, TCR stimulation of the purified memory CD8 T cell subsets also resulted in a rapid increase in the production of GzmB in  $T_{CM}$  and  $T_{SCM}$  cells relative to that in naive T cells (Fig. S3 B). These results provide further evidence that the epigenetic status for the *IFN $\gamma$* , *PRF1*, and *GZMB* genes in human  $T_{CM}$  and  $T_{SCM}$  cells is coupled to the poising of effector molecule expression.

To further assess the ability of the memory CD8 T cell subsets to maintain a “poised-for-expression” gene-expression program during antigen-independent proliferation, we measured the expression of *IFN $\gamma$*  in an in vitro model of cytokine-driven homeostatic cell proliferation. Purified naive and memory CD8 T cell subsets were labeled with the cell proliferation tracking dye CFSE and were then cultured in the presence of the homeostatic cytokines IL-7 and IL-15 for 7 d. Indeed, our results confirm those from prior studies showing that human memory CD8 T cell subsets have a hierarchical capacity to undergo cytokine-driven homeostatic proliferation, with  $T_{SCM}$  cells (Gattinoni et al., 2011) undergoing the most proliferation in the presence of both cytokines (naive <  $T_{EM}$  <  $T_{CM}$  <  $T_{SCM}$ ; Fig. S3, C and D; Sallusto et al., 1999; Gattinoni et al., 2011). We next measured the poised-recall response in cells that had undergone cytokine-driven proliferation by assessing the level of *IFN $\gamma$*  protein in undivided and divided CD8 T cells after TCR stimulation. Quite strikingly, after 7 d in culture with IL-7

and IL-15, divided memory CD8 T cells retained the ability to rapidly express *IFN $\gamma$*  protein after 4 h of TCR stimulation (Fig. 2 A). These results suggest that human memory CD8 T cells retain a gene-expression program during IL-7/IL-15-mediated proliferation that allows the cells to remain poised to elicit a rapid effector response.

#### Effector-associated DNA methylation programs are maintained during in vitro homeostasis

Our WGBS methylation analyses of primary T cells serves as a “snapshot” of the epigenetic state of long-lived memory CD8 T cells but fails to reveal whether the DNA methylation programs are stable during homeostasis. Having validated the DNA methylation status of many DMRs identified from our WGBS analyses, including the DMRs identified in the *IFN $\gamma$*  and *PRF1* loci (Fig. 1 F and Fig. S2), we proceeded to use our newly designed loci-specific assays to determine whether the methylation status would remain unchanged during in vitro, cytokine-driven homeostatic proliferation. Naive,  $T_{EM}$ ,  $T_{CM}$ , and  $T_{SCM}$  CD8 T cell subsets were FACS purified, labeled with CFSE, and maintained in culture with IL-7 and IL-15 for 7 d. After 7 d, we then FACS purified the undivided and divided ( $\geq 3$  rounds of cell division) fraction of cells and measured their DNA methylation status (Fig. 2 B). The *IFN $\gamma$*  locus remained fully demethylated in all memory T cell subsets that had undergone cell division. In contrast, naive CD8 T cells that underwent more than three rounds of division retained a fully methylated *IFN $\gamma$*  locus (Fig. 2 C). These data demonstrate that cell division alone is not sufficient to demethylate the *IFN $\gamma$*  locus in naive cells; rather, the process of demethylation is coupled to additional events/stages of memory T cell differentiation.

Similar to the *IFN $\gamma$*  locus, the demethylated status of CpGs within the *PRF1* locus remained unchanged in dividing CD8  $T_{EM}$  cells (Fig. 2 C). This region of the *PRF1* locus was ~50% demethylated in resting CD8  $T_{CM}$  and  $T_{SCM}$  cells (Fig. 1 F and Fig. S3 E), which enabled us to test whether memory T cells undergo further demethylation through passive mechanisms (i.e., failure to propagate a methylation program during cell division). Remarkably, the 50% methylation status at the CpG sites in the  $T_{CM}$  and  $T_{SCM}$  cells was faithfully propagated for more than three rounds of cell division, demonstrating that acquired epigenetic programs at effector-associated loci can persist during cytokine-driven homeostatic proliferation.

#### CCR7 phenotypic conversion of long-lived $T_{SCM}$ is coupled to changes in DNA methylation during homeostatic proliferation

Antigen-independent phenotypic conversion of memory CD8 T cells has been previously observed during in vivo and in vitro homeostatic proliferation, but it remains openly debated whether this phenotypic conversion represents bona fide reprogramming of the cell’s differentiation state (Wherry et al., 2003; Lefrançois and Marzo, 2006; Gattinoni et al.,

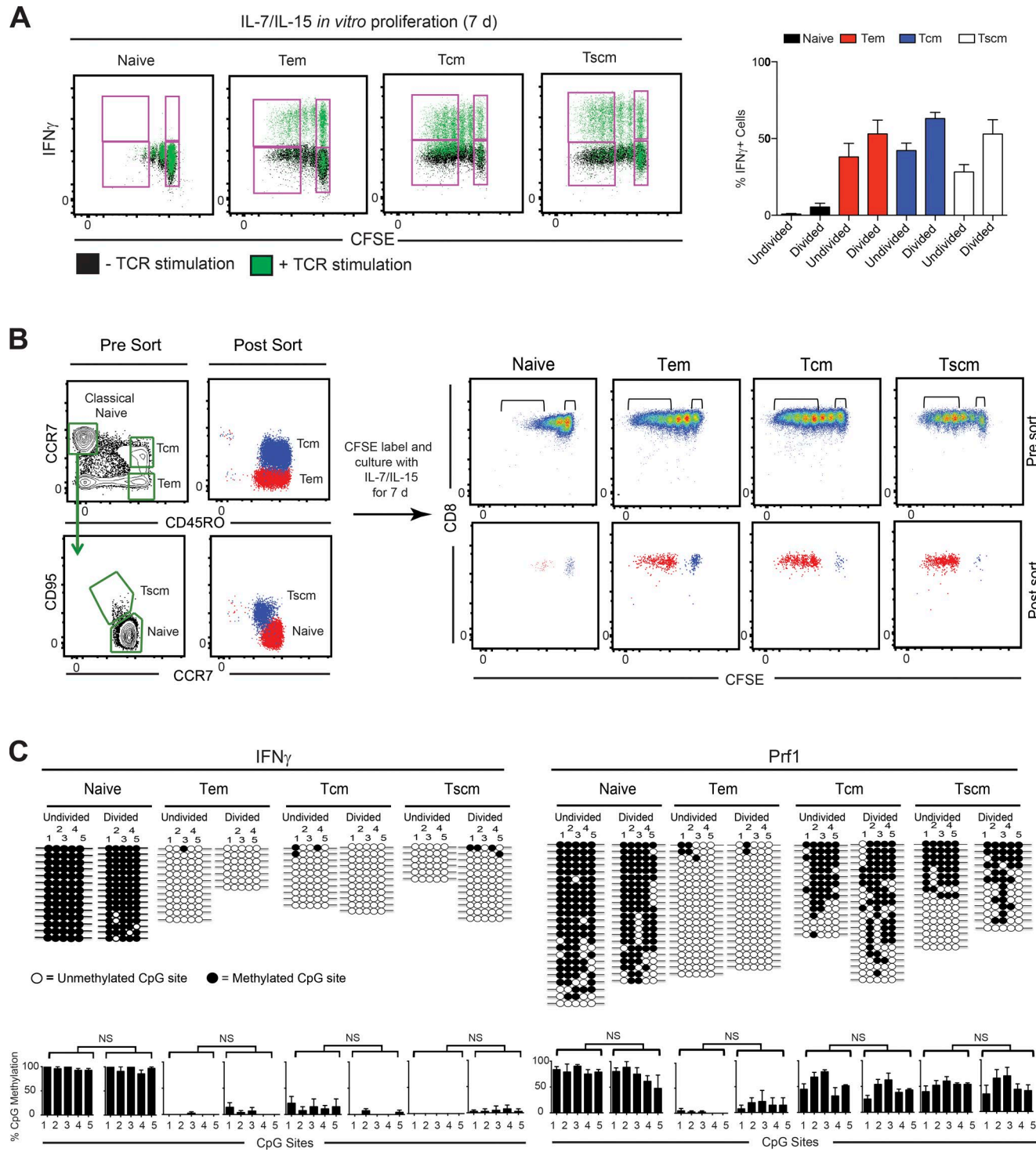


**Figure 2. Stable maintenance of poised effector programs during *in vitro* cytokine-driven proliferation of human memory CD8 T cell subsets.** (A, left) Recall response of undivided and divided, CFSE-labeled, naive,  $T_{EM}$ ,  $T_{CM}$ , and  $T_{SCM}$  CD8 T cells expressing IFN $\gamma$  during exposure to IL-7/IL-15 in culture for 7 d, followed by anti-CD3/CD28 stimulation (1:1 ratio) for 4 h. Gates indicate the percentage of undivided and divided cells. (right) Bar graph showing cumulative data from four independent experiments presented as the percentage means  $\pm$  SEM. CD8 T cells expressing IFN $\gamma$  during homeostatic proliferation after TCR stimulation ( $n = 4$ ). (B) Freshly isolated CD8 T cell subsets were labeled with CFSE and subsequently maintained in culture in the presence of IL-7/IL-15 for 7 d. Undivided and divided cell subpopulations were then sorted, and genomic DNA was extracted for bisulfite sequencing analysis. (C, top) Representative bisulfite sequencing analysis of effector molecules in undivided and divided cells

2011). Indeed, culturing naïve,  $T_{EM}$ ,  $T_{CM}$ , and  $T_{SCM}$  CD8 T cells with IL-7/IL-15 for 7 d results in down-regulation of *CCR7* expression in both  $T_{CM}$  and  $T_{SCM}$  cells and a conversion to  $T_{EM}$ -like cells (Fig. 3, B and C). This observation prompted us to investigate the status of DNA methylation in *CCR7* and CD62L DMRs under those conditions. We first confirmed that the CpG sites in the *CCR7* and CD62L DMRs were fully demethylated in both naïve and  $T_{SCM}$  cells and were significantly methylated in  $T_{EM}$  cells isolated from six independently sorted samples (Fig. 3 A, bottom). Those data further substantiate the link between *CCR7* and CD62L expression and the methylation status of the DMRs. We next measured the methylation status of *CCR7* and CD62L CpGs during cytokine-driven proliferation using the loci-specific assay. Naïve and memory CD8 T cell subsets were again cultured in the presence of IL-7 and IL-15, and the methylation assay was performed on purified undivided and divided populations. Similar to our findings with the *IFN $\gamma$*  and *PRF1* DMRs, the methylation status of the *CCR7* and CD62L DMR CpGs in divided naïve CD8 T cells remained unchanged. However, we detected a significant increase in the methylation levels at the *CCR7* DMR in divided  $T_{SCM}$  cells (Fig. 3 D). These results provide compelling evidence that cytokine-induced developmental changes among long-lived memory CD8 T cells (Gattinoni et al., 2011) are coupled to the cell's ability to undergo selective epigenetic reprogramming. To further assess whether the mechanism(s) regulating the phenotypic and epigenetic conversion of  $T_{SCM}$  and  $T_{CM}$  cells was specific for the *CCR7* locus or was rather a general feature of these cells, we measured CD45RO expression in naïve and memory CD8 T cell after IL-7/IL-15 culture for 7 d. In contrast to *CCR7*, CD45RO expression was not significantly changed after cell division of the naïve and memory CD8 T cell subsets (Fig. S3, C and D). This stability in CD45RO expression was similar to the stability observed with the effector molecules and suggests that homeostasis-induced changes to epigenetic programming in  $T_{CM}$  and  $T_{SCM}$  is restricted to select loci.

A defining feature of long-lived memory CD8 T cells (i.e.,  $T_{CM}$  and  $T_{SCM}$ ) is their enhanced self-renewal compared with shorter-lived memory CD8 T cells ( $T_{EM}$ ). Given that we observed a dichotomy among the pool of  $T_{SCM}$  cells in their ability to retain a *CCR7hi* phenotype during in vitro homeostatic proliferation, we next asked whether down-regulation of *CCR7* expression was associated with a reduced potential to maintain their parental cell identity. *Tcf1* is a transcription factor downstream of the Wnt signaling pathway that has a critical role in regulating CD8 T cell self-renewal (Willinger et al., 2005; Gattinoni et al., 2010). Therefore, we further examined the relationship between *Tcf1* expression (encoded by

the *TCF7* gene) and promoter methylation in freshly isolated naïve and memory CD8 T cells. Indeed, we observed that *Tcf1* expression was inversely correlated with the methylation status of the *TCF7* promoter region (encoding for *Tcf1*; Fig. 4, A and B). We next performed loci-specific methylation profiling of the *TCF7* promoter among the daughter cells that arose from homeostatic proliferation of  $T_{CM}$  and  $T_{SCM}$  CD8 T cells to determine whether their phenotypic interconversion was coupled to stable changes in the epigenetic programs associated with a reduced capacity for self-renewal. Importantly, we observed that the divided  $T_{CM}$  and  $T_{SCM}$  CD8 T cells had indeed down-regulated *Tcf1* protein expression (Fig. 4 C). Furthermore, the down-regulation of *Tcf1* was coupled to an increase in *TCF7* promoter methylation (Fig. 4 D). These data suggest that the interconversion of long-lived memory CD8 T cells into shorter-lived memory CD8 T cells is coupled to epigenetic repression of transcriptional machinery that are critical for self-renewal.

### Memory CD8 T cells maintain effector and tissue homing-associated DNA methylation programs after adoptive transfer into transplant patients

Collectively, the results from our in vitro homeostasis studies established that DNA methylation programs associated with the heightened recall of effector functions are preserved over several rounds of cytokine-driven cell division, whereas programs coupled to homing markers broadly used to delineate memory T cell subsets can be modified. Although the effector-associated epigenetic programs exhibited remarkable stability under conditions of in vitro homeostasis, a lingering question is whether such stability occurs in vivo. One of the main challenges of studying in vivo human T cell homeostasis is the difficulty of tracking and reisolating adoptively transferred T cells from the recipient because of their low frequency in circulation and the lack of congenic markers to distinguish donor versus recipient T cells. To overcome these challenges we took advantage of a novel T cell depletion strategy used at our institution, which selectively depletes CD45RA<sup>+</sup> cells in haploididentical donor grafts for hematopoietic cell transplantation, thereby providing adoptive transfer of numerous donor memory cells at the time of transplantation (Triplett et al., 2015). This infusion of polyclonal total  $T_{CM}$  and  $T_{EM}$  memory T cells provides a unique opportunity to assess the stability of epigenetic programs in human memory CD8 T cells during in vivo homeostatic proliferation.

Using the transplantation protocol, we assessed the stability of DNA methylation programs in memory CD8 T cells that underwent antigen-independent expansion in vivo. Five blood samples from hematopoietic cell transplant recipients were selected for analyses based on the criteria of

for each CD8 T cell subset. (bottom) Bar graph showing the percentage of CpG methylation (means  $\pm$  SEM) at each site of the effector loci in undivided and divided, naïve,  $T_{EM}$ ,  $T_{CM}$ , and  $T_{SCM}$  cells ( $n = 4$  healthy donors). Mann-Whitney *U* test was used.  $P < 0.05$  was considered significant. NS, not significant. Statistical comparison was based on the mean value of all CpG sites.

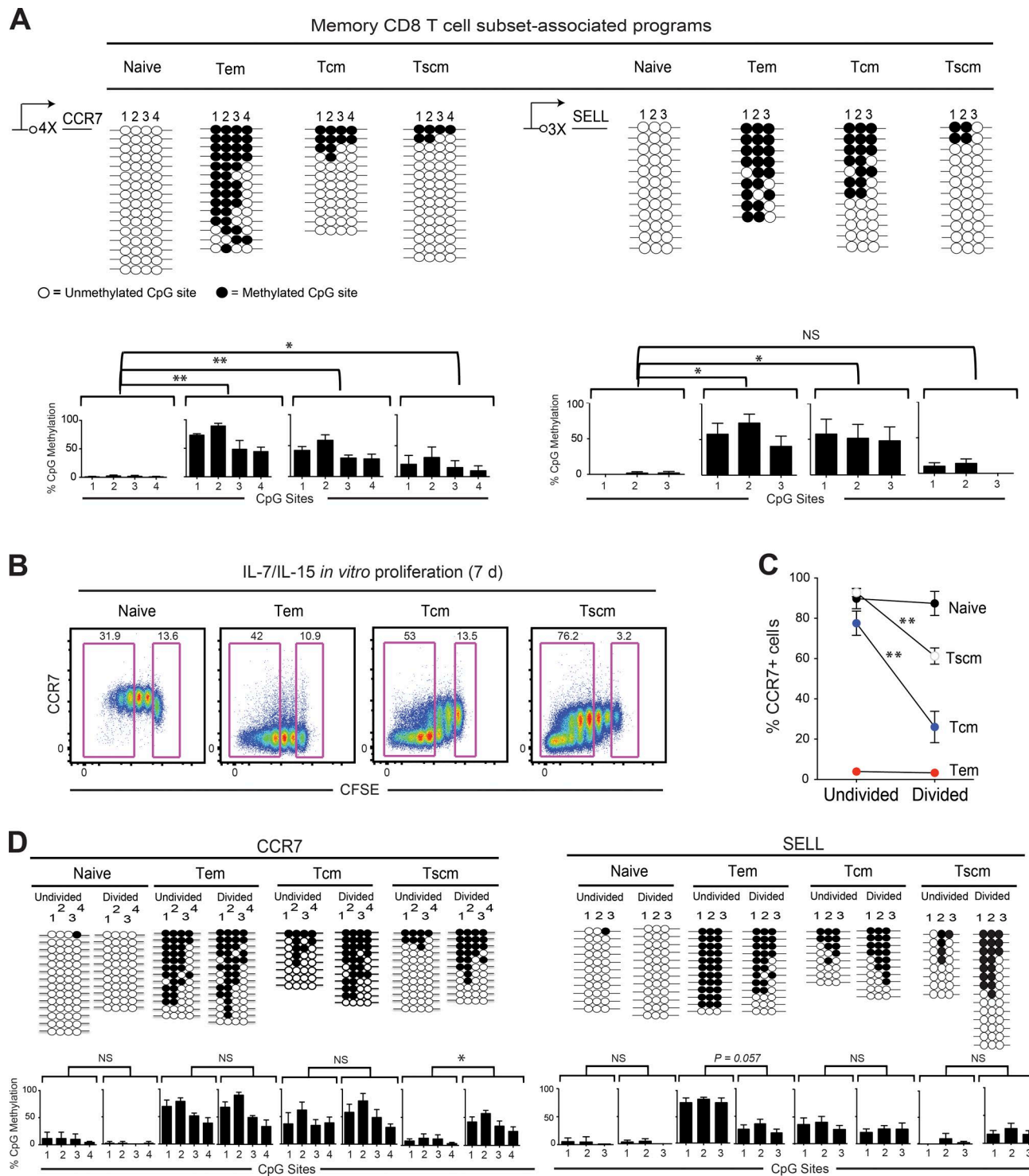


**Figure 3. Plasticity of tissue-homing programs during homeostatic proliferation of human memory CD8 T cell subsets.** (A, top) Representative DNA methylation profile analysis of *CCR7* and *SELL* DMRs from ex vivo isolated CD8 T cell subsets. Each horizontal line represents a clone, and each vertical line represents a CpG site. (bottom) Bar graphs showing the percentage of CpG methylation (means  $\pm$  SEM) for each site ( $n = 4$ –5 independently sorted and analyzed healthy donor samples). Mann-Whitney *U* test was used. \*,  $P < 0.03$ ; and \*\*,  $P < 0.01$  were considered significant. NS, not significant. Statistical comparison was based on the mean value of all CpG sites. (B) *CCR7* expression in undivided and divided, CFSE-labeled, naive,  $T_{EM}$ ,  $T_{CM}$ , and  $T_{SCM}$  CD8 $^{+}$  T cells after exposure to IL-7/IL-15 in culture for 7 d. Gates indicate the percentage of undivided and divided cells ( $n = 4$ ). (C) Paired analysis for *CCR7* expression in undivided and divided populations of naive,  $T_{EM}$ ,  $T_{CM}$ , and  $T_{SCM}$  CD8 $^{+}$  T cells after culture in IL-7/IL-15 for 7 d ( $n = 4$  independently sorted and analyzed healthy donor samples). Paired Student's *t* test was used. \*\*,  $P < 0.01$  was considered significant. Error bars indicate SEM. (D, top) Representative bisulfite

100% donor chimerism among the reconstituted immune cells after infusion, and no signs of immunologic responses to infection (Fig. 5 A). The phenotype of donor T cells was examined before CD45RO enrichment for adoptive transfer and then measured again  $\sim$ 2 mo after adoptive transfer and expansion in the patient. CD8 T cells isolated from the blood of recipients were strikingly void of cells exhibiting a naive phenotype, indicating that enrichment before infusion indeed excluded CD45RO $^{-}$  cells (Fig. 5 A). The expanded CD8 T cells predominantly exhibited a T<sub>EM</sub> phenotype, despite the transfer of both T<sub>CM</sub> and T<sub>EM</sub> memory CD8 T cell (Fig. 5 B, top) and also expressed higher levels of Ki67 indicating that they had recently proliferated (Fig. 5 B, bottom). Notably, the memory CD8 T cells isolated from the recipients retained a high degree of clonal diversity and had only a modest increase in the level of PD-1 expression, further supporting the conclusion that polyclonal expansion of memory T cells in those patients did not occur because of an encounter with pathogen-associated antigens (Fig. 5 C).

Having established that most T cells isolated from the PBMCs of recipients retained a memory phenotype and originated from the donor (chimerism was 100% based on VNTR [variable number tandem repeat]), we next sought to determine the DNA methylation status of effector and homing-associated DMRs in those cells. Loci-specific DNA methylation profiling of the *IFN $\gamma$*  and *PRF1* DMRs in purified donor T<sub>EM</sub> CD8 T cells (pretransfer) and T<sub>EM</sub>-phenotyped cells isolated from the recipients, confirmed that the promoters of those effector-associated genes remained demethylated during in vivo memory T cell reconstitution of the recipients (Fig. 5, D and E). These data unambiguously establish that memory T cells can maintain a transcriptionally permissive epigenetic program at effector-associated loci during in vivo antigen-independent proliferation (Fig. 5 E). Additionally, the *CCR7* and CD62L DMRs were heavily methylated in the recipient memory T cells when compared with the input donor memory T cells (Fig. 5 F). Therefore, despite the donor infusion containing both T<sub>CM</sub> and T<sub>EM</sub> CD8 T cells, the recipient was found to have primarily T<sub>EM</sub> CD8 T cells. It is quite possible that the absence of T<sub>CM</sub>-like CD8 T cells from the circulation of the recipients' samples was due to selective death of the transferred T<sub>CM</sub> or to selective homing to the lymphoid tissue. Yet, a more exciting possibility is that these data represent in vivo evidence of human memory CD8 T cell subset interconversion. Such a conversion of T<sub>CM</sub> CD8 T cells into cells with a T<sub>EM</sub> phenotype is consistent with our in vitro results showing that  $\gamma$ -chain cytokines promote the conversion of long-lived memory CD8 T cells into T<sub>EM</sub> memory CD8 T cells (Fig. 3, B and C).

Over the lifetime of an organism, memory T cell homeostasis ensures protection against previously encountered pathogens and is achieved, in part, by a fine balance between the death and proliferation of those cells (Murali-Krishna et al., 1999; Haas et al., 2011). This balance is largely orchestrated by the common  $\gamma$ -chain cytokines IL-7 (Ladolce et al., 1998; Goldrath et al., 2002), which is essential for cell survival, and IL-15, which promotes cell cycling (Vella et al., 1997; Becker et al., 2002; Tan et al., 2002). Our study establishes that in vivo preservation of effector potential during cytokine-mediated homeostasis of human memory CD8 T cells is coupled to the ability of the cell to propagate acquired DNA methylation programs to newly generated daughter cells. Moreover, these results reveal that stabilization of epigenetic programming occurs in a loci-specific manner, providing new insight into the mechanisms regulating memory T cell subset interconversion (Martin et al., 2015). Broadly, these data highlight epigenetic programming as a mechanism that memory T cells use to strike a balance between remaining adaptive to their current and future environments and retaining a history of past events.

## MATERIALS AND METHODS

### Isolation of human CD8 T cells from healthy donor blood

This study was conducted with approval from the Institutional Review Board (IRB) of St. Jude Children's Research Hospital. PBMCs were collected through the St. Jude Blood Bank, and samples for WGBS were collected under IRB protocol XPD15-086. PBMCs were purified from a platelet-apheresis blood unit using a density gradient. In brief, blood was diluted 1:2.5 using sterile Dulbecco's PBS (Thermo Fisher Scientific). The diluted blood was then overlayed with Ficoll-Paque PLUS medium (GE Healthcare) to a final dilution of 1:2.5 (Ficoll/diluted blood). The gradient was centrifuged at 400 g with no brake for 20 min at room temperature. The PBMC interphase layer was collected, washed with 2% FBS/1 mM EDTA PBS buffer, and centrifuged at 400 g for 5 min. Total CD8 T cells were enriched from PBMCs with the EasySep human CD8 negative-selection kit (STEMCELL Technologies). T cells were collected from the peripheral blood of bone marrow transplant patients enrolled in an IRB-approved protocol (registered at ClinicalTrials.gov, Identifier: NCT01807611). All donors provided informed consent for collection of the blood samples used for the in vivo analyses. Donor chimerism was determined using CLIA-certified VNTR analysis.

sequencing analysis of tissue-homing loci in undivided and divided cells for the indicated CD8 T cell subsets. (bottom) Bar graphs showing the percentage of CpG methylation (means  $\pm$  SEM) for each site of the tissue-homing loci in undivided and divided, naive, T<sub>EM</sub>, T<sub>CM</sub>, and T<sub>SCM</sub> cells ( $n = 5$  independently sorted and analyzed healthy donor samples). Mann-Whitney *U* test was used. \*,  $P < 0.03$  was considered significant. NS, not significant. Statistical comparison was based on the mean value of all CpG sites.

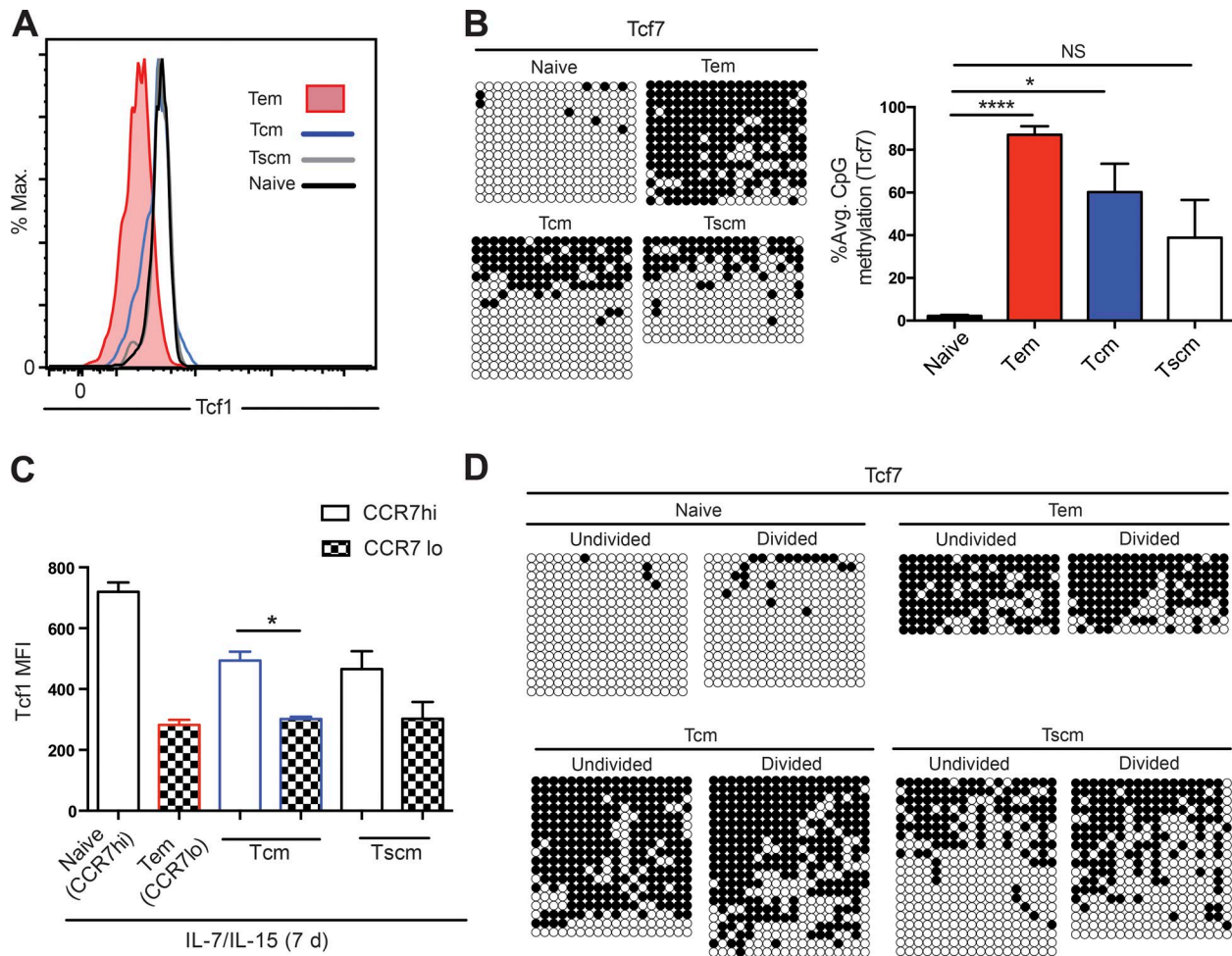


**Figure 4. Tcf1 expression is down-regulated during memory CD8 T cell in vitro homeostatic proliferation.** (A) Histogram showing Tcf1 expression levels in sorted, human, naive,  $T_{EM}$ ,  $T_{CM}$ , and  $T_{SCM}$ . (B, left) Representative bisulfite sequencing analysis of *TCF7* DMR in ex vivo isolated CD8 T cell subsets from one representative donor. Each horizontal line represents a clone, and each vertical line represents a CpG site. (right) Bar graph showing the mean percentage of CpG methylation (means  $\pm$  SEM) for each site ( $n = 3$  healthy donors). \*,  $P < 0.05$ ; and \*\*\*\*,  $P < 0.0001$  were considered significant. Unpaired Student's *t* test was used. Statistical comparison was based on the mean value of all CpG sites. (C) Mean fluorescence intensity (MFI) of Tcf1 in  $CCR7^{lo}$  and  $CCR7^{hi}$  naive and memory CD8 T cell subsets after 7 d of IL-7/IL-15 culture ( $n = 4$  healthy donors). Mann-Whitney *U* test was used. \*,  $P < 0.03$  was considered significant. NS, not significant. Error bars indicate SEM. (D) Representative bisulfite sequencing analysis of *TCF7* in undivided and divided cells for the indicated CD8 T cell subsets.

#### Isolation and flow cytometric analysis of naive and memory CD8 T cell subsets

After enrichment of CD8 T cells, naive and memory CD8 T cell subsets were sorted using the following markers, as previously described (Gattinoni et al., 2011; Lugli et al., 2013). Naive CD8 T cells were phenotyped as live  $CD8^+$ ,  $CCR7^+$ ,  $CD45RO^-$ ,  $CD45RA^+$ , and  $CD95^-$  cells.  $CD8 T_{EM}$  cells were phenotyped as live  $CD8^+$ ,  $CCR7^-$ , and  $CD45RO^+$  cells.  $CD45RA$  staining was included in our analysis to exclude terminally differentiated  $T_{EMRA}$  CD8 T cells, defined as  $CD8^+$ ,  $CCR7^-$ ,  $CD45RO^-$ , and  $CD45RA^+$  cells.  $T_{CM}$  cells were phenotyped as live  $CD8^+$ ,  $CCR7^+$ , and  $CD45RO^+$  cells.  $T_{SCM}$  cells were phenotyped as live  $CD8^+$ ,  $CCR7^+$ ,  $CD45RO^-$ , and  $CD95^+$  cells. Sorted cells were checked for purity (i.e., sam-

ples were considered pure if  $>90\%$  of the cells had the desired phenotype).  $GzmB$  expression was measured in individually sorted naive or memory CD8 T cell subsets that were subsequently stimulated with human CD3/CD28 human T cell activator Dynabeads (Invitrogen) at a 1:1 ratio. After  $\sim 18$  h of incubation at  $37^\circ C$  and 5%  $CO_2$ , cells were harvested for cell-surface staining followed by intracellular staining.

#### Genomic methylation analysis

DNA was extracted from the sorted cells by using a DNA-extraction kit (QIAGEN) and then bisulfite treated using an EZ DNA methylation kit (Zymo Research), which converted all unmethylated cytosines to uracils and protected the methylated cytosines from a deamination reaction. The

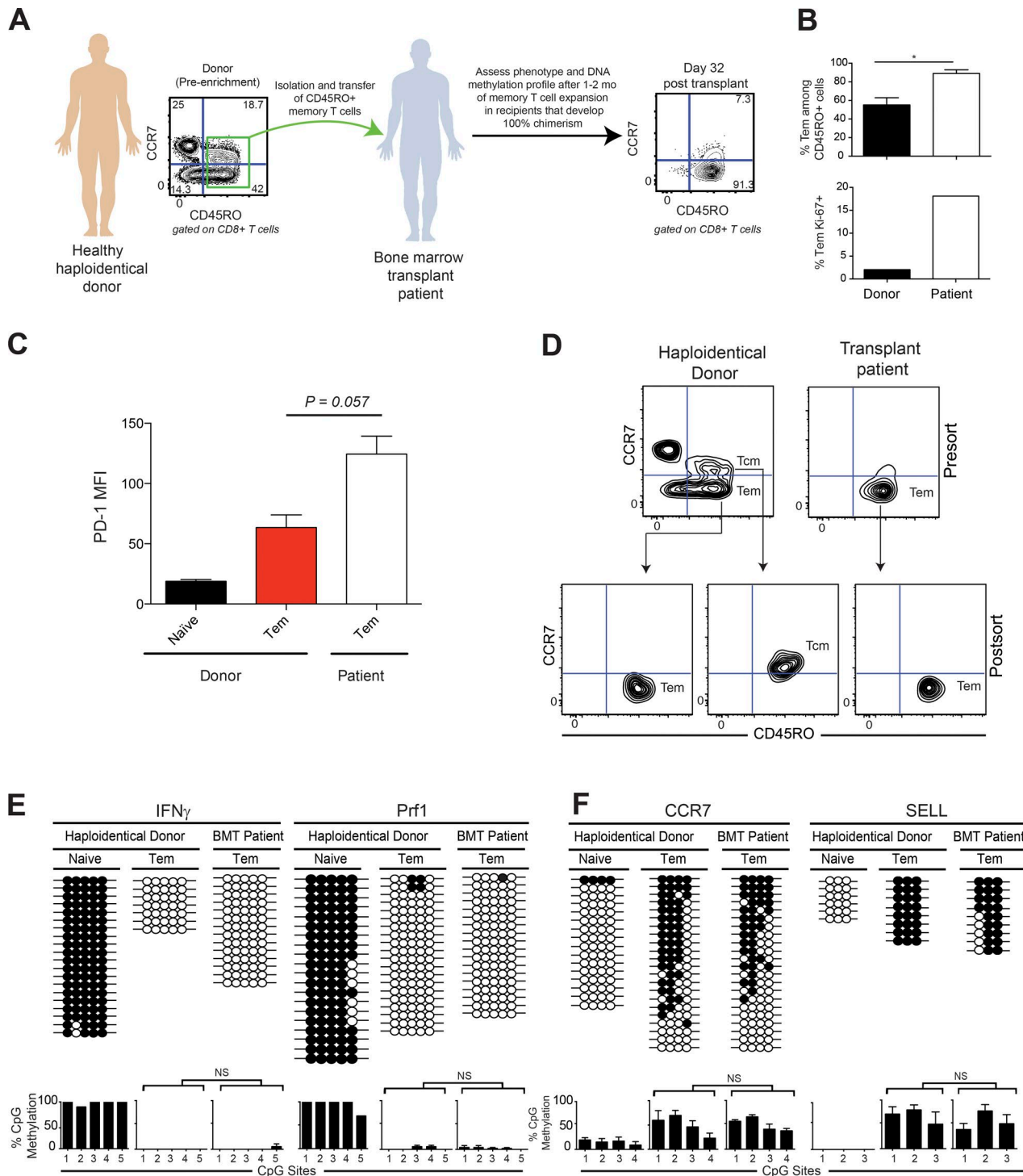


**Figure 5. In vivo stability of effector-associated programs in memory CD8 T cells from immunocompromised patients after donor lymphocyte infusion.** (A) Schematic representation for the donor lymphocyte infusion protocol showing infusion of CD45RO<sup>+</sup> memory T cells from healthy, haploidentical donors into bone marrow transplant (BMT) recipient. Representative FACS plots show the frequency of naive, T<sub>EM</sub>, and T<sub>CM</sub> CD8 T cells in PBMCs from a healthy, haploidentical donor and a patient on day 32 after transplant. (B, top) Bar graph showing the percentage of T<sub>EM</sub> cells among CD45RO<sup>+</sup> CD8 T cells (means  $\pm$  SEM) in donor and bone marrow transplant patient ( $n = 5$ ). (bottom) Ki-67 staining for T<sub>EM</sub> CD8 T cells from a healthy, haploidentical donor and a patient on day 53 after transplant. (C) Mean fluorescence intensity (MFI) of PD-1 in naive and T<sub>EM</sub> CD8 T cells from a healthy, haploidentical donor versus T<sub>EM</sub> from a bone marrow transplant patient ( $n = 4$ ). Error bars indicate SEM. \*,  $P < 0.02$  was considered significant. (D) Representative FACS plots showing pre- and postsort purity for T<sub>EM</sub> and T<sub>CM</sub> in haploidentical donor and transplant patient. (E, top) Representative bisulfite sequencing analysis of

bisulfite-modified DNA-sequencing library was generated using the EpiGnome kit (Epicentre) per the manufacturer's instructions. Bisulfite-modified DNA libraries were sequenced using an Illumina HiSeq system. Sequencing data were aligned to the HG19 genome by using BSMAP software (Xi and Li, 2009). Differential-methylation analysis of CpG methylation among the datasets was determined with a Bayesian hierarchical model to detect regional methylation differences with at least three CpG sites (Wu et al., 2015). To perform loci-specific methylation analysis, bisulfite-modified DNA was PCR amplified with locus-specific primers. The PCR amplicon was cloned into a pGEMT easy vector (Promega) and then transformed into XL10-Gold ultracompetent bacteria (Agilent Technologies). Bacterial colonies were selected using a blue/white X-gal selection system after overnight growth, the cloning vector was then purified from individual colonies, and the genomic insert was sequenced. After bisulfite treatment, the methylated CpGs were detected as cytosines in the sequence, and unmethylated CpGs were detected as thymines in the sequence by using BISMA software (Rohde et al., 2010).

#### In vitro homeostatic proliferation

Sorted naive CD8 T cells and memory CD8 T cell subsets were labeled with CFSE (Life Technologies) at a final concentration of 2  $\mu$ M. CFSE-labeled cells were maintained in culture in RPMI containing 10% FBS, penicillin-streptomycin, and gentamycin-containing IL-7/IL-15 at a final concentration of 25 ng/ml each. After 7 d of incubation at 37°C and 5% CO<sub>2</sub>, undivided and divided cells (third division and higher) were sorted. Sorted cells were checked for purity (>90%). To determine whether the effector-recall response was maintained, we stimulated naive and memory CD8 T cell subsets with anti-CD3/CD28 beads (1:1 ratio) for 4 h in the presence of GolgiStop and GolgiPlug (BD), after a 7 d exposure to IL-7/IL-15 in culture, and then examined the levels of IFN $\gamma$  protein expression by intracellular staining.

#### Quantitative transcriptional analysis

Total RNA was extracted from naive and memory CD8 T cell subsets with the RNeasy plus micro kit (QIAGEN). RNA was reverse transcribed into cDNA with Superscript III reverse transcription (Roche). Real-time PCR was performed on a CFX96 Real-Time System (Bio-Rad Laboratories). Relative quantities of mRNA were determined with the Syber Select Master Mix CFX (Roche). Primer sequences are provided in the Supplemental Materials. The levels of mRNA for each gene were normalized to that of  $\beta$ -actin, and the

fold increase in signal over that of the naive CD8 T cells was determined by the  $\Delta\Delta$ ct calculation.

#### Human primer sequences for loci-specific bisulfite sequencing

*TBX21* forward, 5'-GGTTAGTGTAGTAAAGTTGAGGG-3' and reverse, 5'-CCTCTAAATCCAACATAACCTTCTCC-3'; *EOMES* forward, 5'-ATATGTAGGTGTAGTAGAGAAGAGG-3' and reverse, 5'-CCAAAAACCCTCCCACCTAAAAAAC-3'; *ID2* forward, 5'-GAAATATGTATATAAGTATATTAAAAG-3' and reverse, 5'-CTACCTCAATCTCTACCTCCTTAC-3'; *SELL* forward, 5'-GGTATTATAATTGTATTAAATTTAG-3' and reverse, 5'-CCTATTATATAAAAAAACACTAAATTTC-3'; *CCR7* forward, 5'-GAGAGAATGAAAGTTATTTTTG-3' and reverse, 5'-CTAATTAATACAAAATAAACTATCC-3'; *PD-1* forward, 5'-GCCACAGCAGTGAGCAGAGA-3' and reverse, 5'-CTAAGGATGGGATGAGCCCC-3'; *CD244* (2B4) forward, 5'-GTTTTCAAGGTGTATTAGGGTAAAG-3' and reverse, 5'-CCAAACTCTATAACATCTAAATAAC-3'; *CTLA4* forward, 5'-GGTAAAATTTAATTGGTTGGTGG-3' and reverse, 5'-CTATCCTTCCCTCTAAATCACTTCC-3'; *LAG3* forward, 5'-GGGAGGTTCAGTTGGTTGGTGG-3' and reverse, 5'-CTAACTAATACTACCAAATAACCC-3'; *EZH2* forward, 5'-GTAATATTTACATTGTAGA-3' and reverse, 5'-CCTATTAAATTATCTACTACTAC-3'; *IFN $\gamma$*  forward, 5'-GATTAGAGTAATTGAAATTGTGG-3' and reverse, 5'-CCTCCTCTAACTACTAATATTTATACC-3'; *PRF1* forward, 5'-GTGTGATTATGAGATATGATGTTATATG-3' and reverse, 5'-CCA CTTCCTACTCAACCTACATCCCAC-3'; *TCF7* forward, 5'-AGGGAGTTGTTGATTGTA-3' and reverse, 5'-TCCACAACAACCTAACCCCTAAAAA-3'; and *PTPRC* (CD45RC) forward, 5'-GTTGAGGTTTGTATGG-3' and reverse, 5'-CCTCAACCTCCCAATTATAAC-3'.

#### Online supplemental material

Fig. S1 shows bioinformatics analyses of our genome-wide naive and memory CD8 T cell DNA methylation datasets. Fig. S2 shows loci-specific, bisulfite sequencing DNA methylation validation of various DMRs identified in the WGBS datasets of naive and memory CD8 T cells, including transcription factors and inhibitory receptors. Fig. S3 shows data demonstrating that memory CD8 T cells are poised to elicit effector molecule expression, have demethylated effector loci, and retain CD45RO expression levels during IL-7/IL-15-induced proliferation.

effector-associated loci in donor naive and T<sub>EM</sub> CD8 T cells and BMT patient T<sub>EM</sub> CD8 T cells. (bottom) Bar graph showing the percentage of CpG methylation (means  $\pm$  SEM) for each site of tissue homing-associated loci in naive and T<sub>EM</sub> CD8 T cells from both donor and patient. (F, top) Representative bisulfite sequencing analysis of tissue homing-associated loci in donor naive and T<sub>EM</sub> CD8 T cells and patient T<sub>EM</sub> CD8 T cells. (bottom) Bar graph showing the percentage of CpG methylation (means  $\pm$  SEM) for each site of tissue homing-associated loci in naive and T<sub>EM</sub> CD8 T cells from both donor and patient ( $n = 4$  healthy donors and recipients). Mann-Whitney *U* test was used.

## ACKNOWLEDGMENTS

We thank Drs. Richard Ashmun, Richard Cross, and Greig Lennon of the St. Jude Flow Cytometry and Cell Sorting Facility and the staff of the St. Jude Hartwell Center's Genome Sequencing Facility for all services. We would like to thank Drs. Terrence Geiger and Charles Mullighan for their assistance in obtaining consenting donors for WGBS. We thank Hayden Kissick for helpful discussions on WGBS analyses. We thank Mandy Youngblood and Dr. Angela McArthur for scientific editing, and Drs. J. Scott Hale and Paul G. Thomas for their critical review of our manuscript.

This work was supported by National Institutes of Health grant 1R01AI114442 and by the ALSAC (to B. Youngblood).

The authors declare no competing financial interests.

Submitted: 21 October 2016

Revised: 16 February 2017

Accepted: 4 April 2017

## REFERENCES

Araki, Y., Z. Wang, C. Zang, W.H. Wood III, D. Schones, K. Cui, T.Y. Roh, B. Lhotsky, R.P. Wiersto, W. Peng, et al. 2009. Genome-wide analysis of histone methylation reveals chromatin state-based regulation of gene transcription and function of memory CD8<sup>+</sup> T cells. *Immunity*. 30:912–925. <http://dx.doi.org/10.1016/j.jimmuni.2009.05.006>

Banerjee, A., S.M. Gordon, A.M. Intlekofer, M.A. Paley, E.C. Mooney, T. Lindsten, E.J. Wherry, and S.L. Reiner. 2010. Cutting edge: The transcription factor eomesodermin enables CD8<sup>+</sup> T cells to compete for the memory cell niche. *J. Immunol.* 185:4988–4992. <http://dx.doi.org/10.4049/jimmunol.1002042>

Becker, T.C., E.J. Wherry, D. Boone, K. Murali-Krishna, R. Antia, A. Ma, and R. Ahmed. 2002. Interleukin 15 is required for proliferative renewal of virus-specific memory CD8 T cells. *J. Exp. Med.* 195:1541–1548. <http://dx.doi.org/10.1084/jem.20020369>

Becker, T.C., S.M. Coley, E.J. Wherry, and R. Ahmed. 2005. Bone marrow is a preferred site for homeostatic proliferation of memory CD8 T cells. *J. Immunol.* 174:1269–1273. <http://dx.doi.org/10.4049/jimmunol.174.3.1269>

Bensinger, S.J., M.N. Bradley, S.B. Joseph, N. Zelcer, E.M. Janssen, M.A. Hausner, R. Shih, J.S. Parks, P.A. Edwards, B.D. Jamieson, and P. Tontonoz. 2008. LXR signaling couples sterol metabolism to proliferation in the acquired immune response. *Cell*. 134:97–111. <http://dx.doi.org/10.1016/j.cell.2008.04.052>

Bintu, L., J. Yong, Y.E. Antebi, K. McCue, Y. Kazuki, N. Uno, M. Oshimura, and M.B. Elowitz. 2016. Dynamics of epigenetic regulation at the single-cell level. *Science*. 351:720–724. <http://dx.doi.org/10.1126/science.aab2956>

Charlet, J., C.E. Duymich, F.D. Lay, K. Mundbjerg, K. Dalsgaard Sørensen, G. Liang, and P.A. Jones. 2016. Bivalent regions of cytosine methylation and H3K27 acetylation suggest an active role for DNA methylation at enhancers. *Mol. Cell*. 62:422–431. <http://dx.doi.org/10.1016/j.molcel.2016.03.033>

Chen, T., Y. Ueda, S. Xie, and E. Li. 2002. A novel *Dnmt3a* isoform produced from an alternative promoter localizes to euchromatin and its expression correlates with active de novo methylation. *J. Biol. Chem.* 277:38746–38754. <http://dx.doi.org/10.1074/jbc.M205312200>

Crompton, J.G., M. Narayanan, S. Cuddapah, R. Roychoudhuri, Y. Ji, W. Yang, S.J. Patel, M. Sukumar, D.C. Palmer, W. Peng, et al. 2016. Lineage relationship of CD8<sup>+</sup> T cell subsets is revealed by progressive changes in the epigenetic landscape. *Cell. Mol. Immunol.* 13:502–513. <http://dx.doi.org/10.1038/cmi.2015.32>

Cui, W., Y. Liu, J.S. Weinstein, J. Craft, and S.M. Kaech. 2011. An interleukin-21-interleukin-10-STAT3 pathway is critical for functional maturation of memory CD8<sup>+</sup> T cells. *Immunity*. 35:792–805. <http://dx.doi.org/10.1016/j.jimmuni.2011.09.017>

Denton, A.E., B.E. Russ, P.C. Doherty, S. Rao, and S.J. Turner. 2011. Differentiation-dependent functional and epigenetic landscapes for cytokine genes in virus-specific CD8<sup>+</sup> T cells. *Proc. Natl. Acad. Sci. USA*. 108:15306–15311. <http://dx.doi.org/10.1073/pnas.1112520108>

Fitzpatrick, D.R., K.M. Shirley, and A. Kelso. 1999. Cutting edge: stable epigenetic inheritance of regional IFN- $\gamma$  promoter demethylation in CD44<sup>high</sup>CD8<sup>+</sup> T lymphocytes. *J. Immunol.* 162:5053–5057.

Gattinoni, L., X.S. Zhong, D.C. Palmer, Y. Ji, C.S. Hinrichs, Z. Yu, C. Wrzesinski, A. Boni, L. Cassard, L.M. Garvin, et al. 2009. Wnt signaling arrests effector T cell differentiation and generates CD8<sup>+</sup> memory stem cells. *Nat. Med.* 15:808–813. <http://dx.doi.org/10.1038/nm.1982>

Gattinoni, L., Y. Ji, and N.P. Restifo. 2010. Wnt/ $\beta$ -catenin signaling in T-cell immunity and cancer immunotherapy. *Clin. Cancer Res.* 16:4695–4701. <http://dx.doi.org/10.1158/1078-0432.CCR-10-0356>

Gattinoni, L., E. Lugli, Y. Ji, Z. Pos, C.M. Paulos, M.F. Quigley, J.R. Almeida, E. Gostick, Z. Yu, C. Carpenito, et al. 2011. A human memory T cell subset with stem cell-like properties. *Nat. Med.* 17:1290–1297. <http://dx.doi.org/10.1038/nm.2446>

Goldrath, A.W., P.V. Sivakumar, M. Glaccum, M.K. Kennedy, M.J. Bevan, C. Benoist, D. Mathis, and E.A. Butz. 2002. Cytokine requirements for acute and basal homeostatic proliferation of naive and memory CD8<sup>+</sup> T cells. *J. Exp. Med.* 195:1515–1522. <http://dx.doi.org/10.1084/jem.20020033>

Haas, A., K. Zimmermann, and A. Oxenius. 2011. Antigen-dependent and -independent mechanisms of T and B cell hyperactivation during chronic HIV-1 infection. *J. Virol.* 85:12102–12113. <http://dx.doi.org/10.1128/JVI.05607-11>

Hamann, D., P.A. Baars, M.H. Rep, B. Hooibrink, S.R. Kerkhof-Garde, M.R. Klein, and R.A. van Lier. 1997. Phenotypic and functional separation of memory and effector human CD8<sup>+</sup> T cells. *J. Exp. Med.* 186:1407–1418. <http://dx.doi.org/10.1084/jem.186.9.1407>

Intlekofer, A.M., N. Takemoto, E.J. Wherry, S.A. Longworth, J.T. Northrup, V.R. Palanivel, A.C. Mullen, C.R. Gasink, S.M. Kaech, J.D. Miller, et al. 2005. Effector and memory CD8<sup>+</sup> T cell fate coupled by T-bet and eomesodermin. *Nat. Immunol.* 6:1236–1244. <http://dx.doi.org/10.1038/ni1268>

Intlekofer, A.M., N. Takemoto, C. Kao, A. Banerjee, F. Schambach, J.K. Northrup, H. Shen, E.J. Wherry, and S.L. Reiner. 2007. Requirement for T-bet in the aberrant differentiation of unhelped memory CD8<sup>+</sup> T cells. *J. Exp. Med.* 204:2015–2021. <http://dx.doi.org/10.1084/jem.20070841>

Jones, P.A. 2012. Functions of DNA methylation: islands, start sites, gene bodies and beyond. *Nat. Rev. Genet.* 13:484–492. <http://dx.doi.org/10.1038/nrg3230>

Joshi, N.S., W. Cui, C.X. Dominguez, J.H. Chen, T.W. Hand, and S.M. Kaech. 2011. Increased numbers of preexisting memory CD8 T cells and decreased T-bet expression can restrain terminal differentiation of secondary effector and memory CD8 T cells. *J. Immunol.* 187:4068–4076. <http://dx.doi.org/10.4049/jimmunol.1002145>

Kaech, S.M., J.T. Tan, E.J. Wherry, B.T. Konieczny, C.D. Surh, and R. Ahmed. 2003. Selective expression of the interleukin 7 receptor identifies effector CD8 T cells that give rise to long-lived memory cells. *Nat. Immunol.* 4:1191–1198. <http://dx.doi.org/10.1038/ni1009>

Katan-Khaykovich, Y., and K. Struhl. 2002. Dynamics of global histone acetylation and deacetylation in vivo: Rapid restoration of normal histone acetylation status upon removal of activators and repressors. *Genes Dev.* 16:743–752. <http://dx.doi.org/10.1101/gad.967302>

Lefrançois, L., and A.L. Marzo. 2006. The descent of memory T-cell subsets. *Nat. Rev. Immunol.* 6:618–623. <http://dx.doi.org/10.1038/nri1866>

Lefrançois, L., and D. Masopust. 2002. T cell immunity in lymphoid and non-lymphoid tissues. *Curr. Opin. Immunol.* 14:503–508. [http://dx.doi.org/10.1016/S0952-7915\(02\)00360-6](http://dx.doi.org/10.1016/S0952-7915(02)00360-6)

Lodolce, J.P., D.L. Boone, S. Chai, R.E. Swain, T. Dassopoulos, S. Tretin, and A. Ma. 1998. IL-15 receptor maintains lymphoid homeostasis by

supporting lymphocyte homing and proliferation. *Immunity*. 9:669–676. [http://dx.doi.org/10.1016/S1074-7613\(00\)80664-0](http://dx.doi.org/10.1016/S1074-7613(00)80664-0)

Lugli, E., L. Gattinoni, A. Roberto, D. Mavilio, D.A. Price, N.P. Restifo, and M. Roederer. 2013. Identification, isolation and in vitro expansion of human and nonhuman primate T stem cell memory cells. *Nat. Protoc.* 8:33–42. <http://dx.doi.org/10.1038/nprot.2012.143>

Martin, M.D., M.T. Kim, Q. Shan, R. Sompallae, H.H. Xue, J.T. Harty, and V.P. Badovinac. 2015. Phenotypic and functional alterations in circulating memory CD8 T cells with time after primary infection. *PLoS Pathog.* 11:e1005219. <http://dx.doi.org/10.1371/journal.ppat.1005219>

Masopust, D., V. Vezys, A.L. Marzo, and L. Lefrançois. 2001. Preferential localization of effector memory cells in nonlymphoid tissue. *Science*. 291:2413–2417. <http://dx.doi.org/10.1126/science.1058867>

Murali-Krishna, K., L.L. Lau, S. Sambhara, F. Lemonnier, J. Altman, and R. Ahmed. 1999. Persistence of memory CD8 T cells in MHC class I-deficient mice. *Science*. 286:1377–1381. <http://dx.doi.org/10.1126/science.286.5443.1377>

Pearce, E.L., A.C. Mullen, G.A. Martins, C.M. Krawczyk, A.S. Hutchins, V.P. Zediak, M. Banica, C.B. DiCioccio, D.A. Gross, C.A. Mao, et al. 2003. Control of effector CD8<sup>+</sup> T cell function by the transcription factor eomesodermin. *Science*. 302:1041–1043. <http://dx.doi.org/10.1126/science.1090148>

Pipkin, M.E., J.A. Sacks, F. Cruz-Guilloty, M.G. Lichtenheld, M.J. Bevan, and A. Rao. 2010. Interleukin-2 and inflammation induce distinct transcriptional programs that promote the differentiation of effector cytolytic T cells. *Immunity*. 32:79–90. <http://dx.doi.org/10.1016/j.immuni.2009.11.012>

Plotkin, S., W. Orenstein, and P. Offit. 2013. *Vaccines*. Sixth edition. Elsevier, Philadelphia. 1570 pp.

Rohde, C., Y. Zhang, R. Reinhardt, and A. Jeltsch. 2010. BISMA--fast and accurate bisulfite sequencing data analysis of individual clones from unique and repetitive sequences. *BMC Bioinformatics*. 11:230. <http://dx.doi.org/10.1186/1471-2105-11-230>

Russ, B.E., M. Olshansky, H.S. Smallwood, J. Li, A.E. Denton, J.E. Prier, A.T. Stock, H.A. Croom, J.G. Cullen, M.L. Nguyen, et al. 2014. Distinct epigenetic signatures delineate transcriptional programs during virus-specific CD8<sup>+</sup> T cell differentiation. *Immunity*. 41:853–865. (published erratum appears in *Immunity*. 2014. 41:1064) <http://dx.doi.org/10.1016/j.immuni.2014.11.001>

Sallusto, F., D. Lenig, R. Förster, M. Lipp, and A. Lanzavecchia. 1999. Two subsets of memory T lymphocytes with distinct homing potentials and effector functions. *Nature*. 401:708–712. <http://dx.doi.org/10.1038/44385>

Tan, J.T., B. Ernst, W.C. Kieper, E. LeRoy, J. Sprent, and C.D. Surh. 2002. Interleukin (IL)-15 and IL-7 jointly regulate homeostatic proliferation of memory phenotype CD8<sup>+</sup> cells but are not required for memory phenotype CD4<sup>+</sup> cells. *J. Exp. Med.* 195:1523–1532. <http://dx.doi.org/10.1084/jem.20020066>

Thaventhiran, J.E., D.T. Fearon, and L. Gattinoni. 2013. Transcriptional regulation of effector and memory CD8<sup>+</sup> T cell fates. *Curr. Opin. Immunol.* 25:321–328. <http://dx.doi.org/10.1016/j.co.2013.05.010>

Thomas, R.M., C.J. Gamper, B.H. Ladle, J.D. Powell, and A.D. Wells. 2012. De novo DNA methylation is required to restrict T helper lineage plasticity. *J. Biol. Chem.* 287:22900–22909. <http://dx.doi.org/10.1074/jbc.M111.312785>

Triplett, B.M., D.R. Shook, P. Eldridge, Y. Li, G. Kang, M. Dallas, C. Hartford, A. Srinivasan, W.K. Chan, D. Suwannasaen, et al. 2015. Rapid memory T-cell reconstitution recapitulating CD45RA-depleted haploididentical transplant graft content in patients with hematologic malignancies. *Bone Marrow Transplant.* 50:1012. <http://dx.doi.org/10.1038/bmt.2015.139>

Tzelepis, F., J. Joseph, E.K. Haddad, S. Maclean, R. Dudani, F. Agenes, S.L. Peng, R.P. Sekaly, and S. Sad. 2013. Intrinsic role of FoxO3a in the development of CD8<sup>+</sup> T cell memory. *J. Immunol.* 190:1066–1075. <http://dx.doi.org/10.4049/jimmunol.1200639>

Veiga-Fernandes, H., U. Walter, C. Bourgeois, A. McLean, and B. Rocha. 2000. Response of naïve and memory CD8<sup>+</sup> T cells to antigen stimulation in vivo. *Nat. Immunol.* 1:47–53. <http://dx.doi.org/10.1038/76907>

Vella, A., T.K. Teague, J. Ihle, J. Kappler, and P. Marrack. 1997. Interleukin 4 (IL-4) or IL-7 prevents the death of resting T cells: Stat6 is probably not required for the effect of IL-4. *J. Exp. Med.* 186:325–330. <http://dx.doi.org/10.1084/jem.186.2.325>

Weng, N.P., Y. Araki, and K. Subedi. 2012. The molecular basis of the memory T cell response: Differential gene expression and its epigenetic regulation. *Nat. Rev. Immunol.* 12:306–315. <http://dx.doi.org/10.1038/nri3173>

Wherry, E.J., V. Teichgräber, T.C. Becker, D. Masopust, S.M. Kaech, R. Antia, U.H. von Andrian, and R. Ahmed. 2003. Lineage relationship and protective immunity of memory CD8 T cell subsets. *Nat. Immunol.* 4:225–234. <http://dx.doi.org/10.1038/ni889>

Willinger, T., T. Freeman, H. Hasegawa, A.J. McMichael, and M.F. Callan. 2005. Molecular signatures distinguish human central memory from effector memory CD8 T cell subsets. *J. Immunol.* 175:5895–5903. <http://dx.doi.org/10.4049/jimmunol.175.9.5895>

Wong, P., and E.G. Pamer. 2001. Cutting edge: Antigen-independent CD8 T cell proliferation. *J. Immunol.* 166:5864–5868. <http://dx.doi.org/10.4049/jimmunol.166.10.5864>

Wu, H., T. Xu, H. Feng, L. Chen, B. Li, B. Yao, Z. Qin, P. Jin, and K.N. Conneely. 2015. Detection of differentially methylated regions from whole-genome bisulfite sequencing data without replicates. *Nucleic Acids Res.* 43:e141. <http://dx.doi.org/10.1093/nar/gkv715>

Xi, Y., and W. Li. 2009. BSMAP: Whole genome bisulfite sequence MAPping program. *BMC Bioinformatics*. 10:232. <http://dx.doi.org/10.1186/1471-2105-10-232>

Zimmermann, C., A. Prévost-Blondel, C. Blaser, and H. Pircher. 1999. Kinetics of the response of naive and memory CD8 T cells to antigen: similarities and differences. *Eur. J. Immunol.* 29:284–290. [http://dx.doi.org/10.1002/\(SICI\)1521-4141\(199901\)29:01<284::AID-IMMU284>3.0.CO;2-C](http://dx.doi.org/10.1002/(SICI)1521-4141(199901)29:01<284::AID-IMMU284>3.0.CO;2-C)